Eur. J. Biochem. **266**, 484–492 (1999) © FEBS 1999

Conformations in solution of the fuscopeptins

Phytotoxic metabolites of *Pseudomonas fuscovaginae*

Simona Baré[1], Vincenza M. Coiro[1,3], Andrea Scaloni[2], Alfredo Di Nola[3], Maurizio Paci[4*], Anna L. Segre[1] and Alessandro Ballio[5]

[1]*Istituto di Strutturistica Chimica 'G. Giacomello', CNR, Montelibretti, Italy;* [2]*IABBAM e Centro Internazionale Servizi di Spettrometria di Massa, CNR-Università 'Federico II', Napoli, Italy;* [3]*Dipartimento di Chimica, Università di Roma 'La Sapienza', Italy;* [4]*Dipartimento di Scienze e Tecnologie Chimiche, Università 'Tor Vergata', Roma, Italy;* [5]*Dipartimento di Scienze Biochimiche 'A. Rossi Fanelli', Università 'La Sapienza' e Centro di Biologia Molecolare del CNR, Roma, Italy*

Fuscopeptins are phytotoxic amphiphilic lipodepsipeptides containing 19 amino acid residues. They are produced by the plant pathogenic bacterium *Pseudomonas fuscovaginae* in two forms, A and B, which differ only in the number of methylene groups in the fatty acid chain. Their covalent structure and biological properties have been reported previously. CD and NMR spectroscopy investigations in solution revealed the absence of identifiable elements of secondary and tertiary structure for these molecules. Fuscopeptin B appears to be completely unstructured in aqueous solution, and has a large molecular flexibility. A dramatic conformational change was observed upon addition of trifluoroethanol. This study reports the complete interpretation of the two-dimensional NMR spectra and the NOE results obtained for fuscopeptin B in water/trifluoroethanol solutions; the signals relative to the peptidic moiety are identical to those observed for fuscopeptin A. The results of this investigation were used to determine the solution structure of fuscopeptin B by computer simulations applying distance geometry and simulated annealing procedures. In water/trifluoroethanol solutions the peptidic region appears to have a partly helical structure. The lactonic ring assumes defined conformations very similar to those already reported for other lipodepsipeptides. The structure for fuscopeptin B in solution is also valid for fuscopeptin A because of the negligible structural difference between the two metabolites.

Keywords: fuscopeptins; lipodepsipeptides; molecular dynamics; NMR; phytotoxins.

Many plant pathogenic pseudomonads synthesize in culture two groups of lipodepsipeptides that differ from each other in the size of the peptide moiety and the nature of the amino acid residues as well as in the lipid moiety [1]. Similarly, the recently investigated *Pseudomonas fuscovaginae*, a pathogen of rice and other graminae, produces the 'small' syringotoxin [2], an already known nonapeptide, and the 'large' fuscopeptins A and B (fuscopeptins), new 19 amino-acid-containing peptides [3]. The covalent structure of the fuscopeptins are shown in Fig. 1. They share many structural and biological features with tolaasin [4], syringopeptins [5] and corpeptins [1], 'large' lipodepsipeptides isolated from other pseudomonads. A comparison of their structures is made in Table 1.

The three-dimensional molecular characterization of one syringopeptin (SP-25A) has been completed recently with determination of the solution conformation in solution by NMR spectroscopy and computer simulations applying distance geometry and molecular dynamics procedures [6]. Here the same approach has been used for determining the solution conformation of fuscopeptin B, the results reported include the complete interpretation of two-dimensional NMR spectra in different concentrations of aqueous trifluoroethanol; the experimentally observed NOEs have been integrated and used as restraints in the molecular simulations. These results are valid also for fuscopeptin A which differs from fuscopeptin B only in having two fewer methylene groups in the fatty acid chain, as shown in Fig. 1. Finally, similarities and differences of the solution structures found for fuscopeptin B and for some of the previously examined lipodepsipeptides are discussed.

Correspondence to M. Paci, Dipartimento di Scienze e Tecnologie Chimiche, Università 'Tor Vergata', Via Ricerca Scientifica 1, 00133 Roma, Italy.

Abbreviations: A_2bu, 2,4-diaminobutanoic acid; Dhb, (*Z*)-2,3-dehydro-2-aminobutanoic acid; DG-SA, distance geometry-simulated annealing.

Dedication: this paper is dedicated to the memory of our colleague Professor Giacomino Randazzo.

(Received 7 July 1999, revised 21 September 1999, accepted 22 September 1999)

MATERIALS AND METHODS

Preparation and purification of fuscopeptins

P. fuscovaginae strain UPB264 was used throughout. Growth of the organism, extraction of cultures and fractionation of the bioactive metabolites were performed by reverse-phase HPLC as reported previously [2,3].

CD

The spectropolarimeter and the experimental conditions were the same as those used previously [6].

NMR spectroscopy

The ^{1}H-NMR spectra of samples (approximately 0.8 mg·mL^{-1}) were run at a temperature of 27 °C on a Bruker AMX600 instrument operating at 600.14 MHz. They were performed in

Table 1. Comparison of the amino acid moiety of pseudomonad peptins. In all of the compounds listed the lactone closure is between the C-terminal residue and the *allo*-T residue. Identical or closely related residues are in bold. References are indicated in the last column in brackets. FA, fatty acid.

Fuscopeptins	**FA**	**Dhb**	**P**	**L**	**A**	**A**	**A**	**A**	**V**	–	–	–	G	**A**	**V**	**A**	**V**	**Dhb**	***allo*-T**	–	–	–	A	**A_2bu**	**A_2bu**	**F**	[3]
Corpeptins	**FA**	**Dhb**	**P**	**A**	**A**	**A**	**V**	**V**	Dhb	Hse	**V**	***allo*-I**	**Dhb**	**A**	**A**	**A**	**V**	**Dhb**	***allo*-T**	–	–	–	A	**A_2bu**	S	**I**	[1]
Syringopeptin 25A	**FA**	**Dhb**	**P**	**V**	**A**	**A**	**V**	**L**	**A**	**A**	Dhb	**V**	**Dhb**	**A**	**V**	**A**	**A**	**Dhb**	***allo*-T**	S	**A**	V	A	**A_2bu**	**A_2bu**	**Y**	[5]
Syringopeptin 22A	**FA**	**Dhb**	**P**	**V**	**V**	**A**	**A**	**V**	**V**	–	–	–	**Dhb**	**A**	**V**	**A**	**A**	**Dhb**	***allo*-T**	S	**A**	Dhb	A	**A_2bu**	**A_2bu**	**Y**	[5]
Syringopeptin sugar cane	**FA**	**Dhb**	**P**	**V**	**L**	**A**	**A**	**L**	**V**	–	–	–	**Dhb**	**A**	**V**	**A**	**A**	**Dhb**	***allo*-T**	S	**A**	Dhb	A	**A_2bu**	**A_2bu**	**Y**	[27]
Tolaasin	**FA**	**Dhb**	**P**	**S**	**L**	**V**	S	**L**	**V**	**V**	**Q**	**L**	V	–	–	–	–	**Dhb**	**allo-T**	–	–	–	I	Hse	**A_2bu**	**K**	[4]

water and in aqueous deuterated 2,2,2-trifluoroethanol (50 and 80% trifluoroethanol; v/v). Some spectra were also performed at a concentration of 0.4 mg·mL^{-1} to exclude concentration effects due to peptide aggregation. Two-dimensional TOCSY and ROESY experiments were performed by the pulse sequences [7–9] in phase sensitive modality [10]. FIDs were collected over 1 K of memory for 512 increments. After a resolution enhancement with a sine bell function shifted by p/3, a zero filling was introduced to obtain a 1 K × 1 K real matrix. In the ROESY spectra a spinlock mixing time of 0.080 s was applied. In TOCSY experiments using a MLEV-17 spinlock sequence [11] a mixing time of 0.1 s was applied to obtain remote scalar connectivities. In all cases a relaxation delay of 2.0 s before the pulse sequence was applied.

Computer simulations

Distance geometry-simulated annealing procedure (DG-SA). DG-SA energy minimization and the subsequent analysis of the structures were performed by the program XPLOR version 3.1 [12]. The calculations were based on the hybrid DG-SA protocol [13–15], using the force field included in XPLOR for DG-SA calculations. Further refinements were performed with the CHARMM empirical energy function [16,17]. Interproton distance restraints were estimated from two-dimensional NOESY spectra. All NOEs were classified into three groups as strong, medium or weak and given upper limits r_{ij} = 0.32, 0.40 and 0.50 nm, respectively [18], according to previous calculations on other lipodepsipeptides [6,19,20]. When possible, stereospecific assignments of prochiral methylene protons or methyl groups were made. This was accomplished removing distance constraints for prochiral hydrogens or groups, running distance geometry to produce a set of structures and using NOE information to select one proton, or methyl group, rather than the other. When all NOEs always favoured the same stereospecific assignment, the assignment was considered to be valid. Otherwise the pseudoatom representation was used and an additional distance term of 0.05 nm was added to the upper distance bounds. To simulate the water/trifluoroethanol mixture solvent, the dielectric constant ε was set to a value of 10. The peptidic torsion angles were restrained in the *trans* conformation by adding a proper dihedral potential. A restraining potential for the χ angle of the two 2,3-dehydro-2-aminobutanoic (Dhb) residues was included to maintain the *Z* conformation.

According to the procedure proposed by Nilges *et al.* [15] and to previous calculations performed on related lipodepsipeptides [6,19,20], we used 100 cycles of Powell minimization [21] of van der Waals', bond and NOE terms and 100 subsequent cycles of the bond angle terms to improve the covalent geometry of the embedded structures. They were followed by a molecular dynamics simulation stage, starting at a temperature of 2000 K, to introduce the chirality and planarity. The correct chirality of the structure was established on the basis of the lowest energy of the embedded structures. The subsequent stage was the cooling of the structures to a final temperature of 100 K with increased van der Waals' terms. Finally, 200 steps of Powell minimization of the structures were performed. The structures obtained were then refined by a further simulated annealing stage consisting of 1000 steps of molecular dynamics calculation at 2000 K and then of 1000 cooling steps to a final temperature of 100 K. The van der Waals' interactions were softened to enable atoms to move through each other. The structures obtained were then subjected to 100 cycles of energy minimization using the conjugated gradients of the Powell algorithm. The criteria of acceptance adopted for the generated conformations were: deviation of the actual distance, r_{ij}, from the experimental upper distance, r_{ij}^+, determined by the NOE intensity, $r_{ij} < r_{ij}^+ + 0.05$ nm; rms difference for the covalent bond deviations from ideality < 0.001 nm; rms difference for bond angle deviations from ideality $< 2°$.

RESULTS

As in other structural studies of peptides and proteins bidimensional NMR experiments gave a number of experimentally determined interproton distance (NOEs) for use as constraints in computer simulation. The intrinsically high internal mobility of fuscopeptins causes problems in the computational procedure of molecular simulation. The simulation of these phytotoxic lipodepsipeptides from NMR data is complicated further by: the presence of side-chain modified amino acids; the presence of a hydrophobic fatty acid chain; alternation of chirality along the sequence; and by the conformational complication caused by the lactonic ring

R-*Z*Dhb-*D*Pro-*L*Leu-*D*Ala-*D*Ala-*D*Ala-*D*Ala-*D*Val-Gly-*D*Ala-*D*Val-*D*Ala-*D*Val-*Z*Dhb-*Dallo*-Thr-*L*Ala-*L*A2bu-*D*A2bu-*L*-Phe

FP-A : R= CH_3-$(CH_2)_4$-CHOH-CH_2-CO-

FP-B : R= CH_3-$(CH_2)_6$-CHOH-CH_2-CO-

Fig. 1. Chemical structure of fuscopeptins A and B. The lactone closure is between the C-terminal residue and the *allo*-Thr residue.

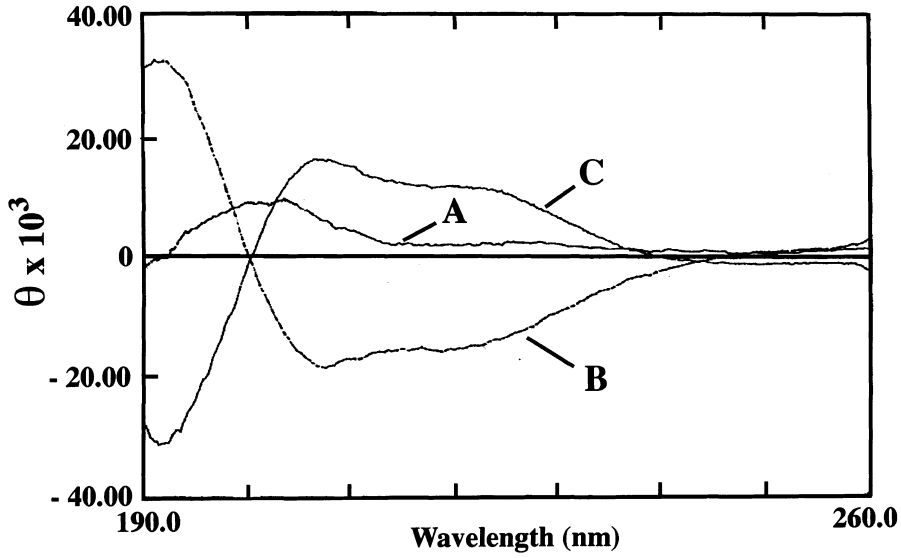

Fig. 2. CD spectra of fuscopeptin B in the far-UV region. (A) Water solution (solid line); (B) 80% aqueous trifluoroethanol (dashed line); (C) the peptide bombinin [26] which is in a right-handed α-helical form in 80% aqueous trifluoroethanol.

closure. Many of these structural elements are surprisingly well conserved (Table 1). Detailed knowledge of the relationship between the bioactive properties and the conformational similarity in the solution structure of various lipodepsipeptides awaits further elucidation. In addition, the influence of all the above mentioned structural elements on the solution conformation of this class of compounds is has not been elucidated completely.

NMR spectroscopy

The structure of fuscopeptins described previously by Ballio *et al.* [3] and reported in Fig. 1 was corroborated by more accurate NMR spectroscopic measurements. For the identical peptide moiety of the two fuscopeptins (they only differ from each other for the length of the 3-hydroxyacyl moiety) the conformational study was limited to the major component B. The NMR spectrum of fuscopeptin B in aqueous solution was characteristic of a peptide with a completely unstructured conformation. The spectrum resulted, in practice, from the sum of the resonances due to constituent amino acids devoid of the dispersion usually produced by elements of secondary and/or tertiary structure. These results were in perfect agreement with CD spectra of fuscopeptin B in water (Fig. 2) which lacks recognizable elements of secondary structure. Addition of trifluoroethanol, which mimicks a membrane-like environment, induced a conformational change suggesting an increased level of helical folding. Therefore, the two-dimensional NMR spectroscopy experiments were performed in aqueous TFE solutions with 50 and 80% trifluoroethanol, respectively. In these conditions, all of the resonances were dispersed and the spectral assignments were made easier; in particular TOCSY spectra gave the correlations of the amino acid residues leading to a clear identification of the spin systems.

In detail, the seven Ala, the three Val, the Gly and the Thr residues have been assigned due to their well recognizable spin systems and the characteristic chemical shift values. The two Dhb gave a singlet NH. Leu, Phe and Pro were recognized from their spin systems.

NOESY experiments did not give useful cross-peaks due to the small molecular weight of the compound which gives an unfavourable correlation time. Conversely, ROESY performed under the same conditions led to the collection of a number of

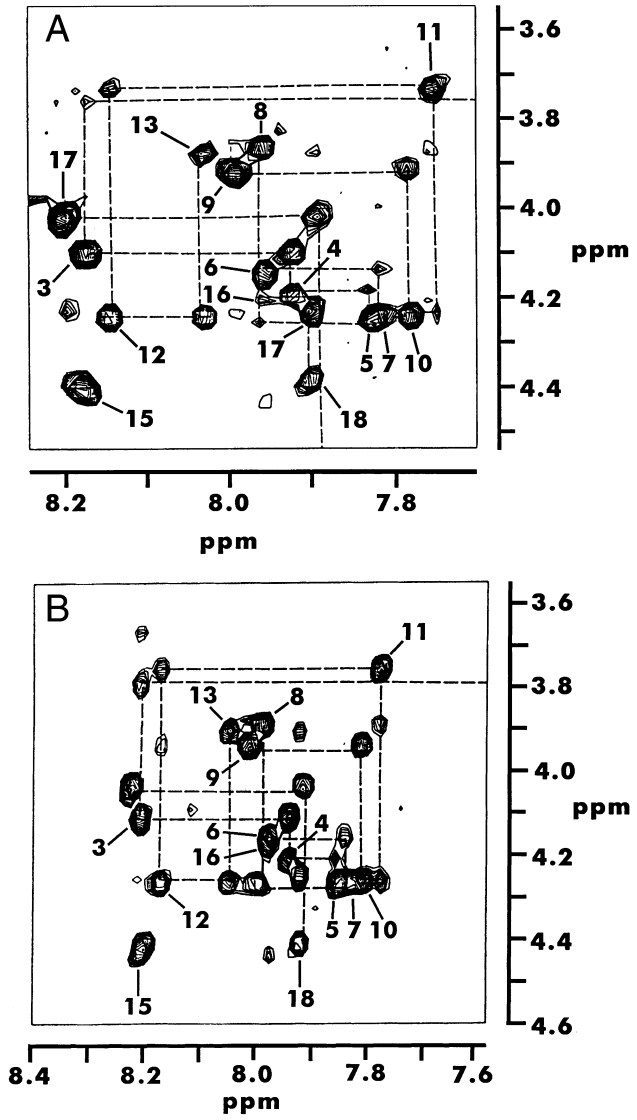

Fig. 3. Fingerprint region of ROESY spectra of fuscopeptin B in aqueous/trifluoroethanol solutions obtained with a spinlock time of 0.2 s. (A) Spectrum in 50% aqueous trifluoroethanol; (B) spectrum in 80% aqueous trifluoroethanol.

Table 2. Assignments of the resonances of the NMR spectrum of fuscopeptin B in 80% aqueous trifluoroethanol. Values reported in parentheses are those observed in 50% aqueous trifluoroethanol. Fuscopeptin B fatty acid chemical shift values (p.p.m.): C2, 2.58 (2.59); C3, 4.12 (4.12); C4, 1.37 (1.38); C5, 1.59 (1.61); C6–C7, 1.46 (1.48); C8, 1.33 (1.33); C9, 1.27 (1.34); C10, 0.90 (0.90).

	Chemical shift (p.p.m.)				
Residue assignment	NH	CHα	CHβ,β′	CHγ,γ′	CHδ,δ′
Dhb1	9.05		5.80		
	(9.06)		(5.81)		
Pro2		4.41	2.39	2.00	3.77, 3.67
		(4.42)	(2.39)	(2.01)	(3.66, 3.78)
Leu3	8.19	4.10	1.97, 1.81		0.96
	(8.20)	(4.10)	(1.98, 1.81)		(0.97)
Ala4	7.94	4.19	1.48		
	(7.84)	(4.19)	(1.47)		
Ala5	7.83	4.24	1.56		
	(7.83)	(4.25)	(1.57)		
Ala6	7.96	4.13	1.51		
	(7.97)	(4.14)	(1.52)		
Ala7	7.83	4.25	1.56		
	(7.84)	(4.26)	(1.57)		
Val8	7.97	3.87	2.21	1.04, 1.11	
	(7.97)	(3.87)	(2.20)	(1.03, 1.13)	
Gly9	7.99	3.91			
	(8.01)	(3.94)			
Ala10	7.78	4.23	1.56		
	(7.80)	(4.25)	(1.57)		
Val11	7.76	3.72	2.26	0.98, 1.11	
	(7.77)	(3.75)	(2.28)	(1.01, 1.10)	
Ala12	8.14	4.24	1.60		
	(8.15)	(4.25)	(1.62)		
Val13	8.02	3.87	2.38	1.08, 1.18	
	(8.04)	(3.89)	(2.38)	(1.08, 1.18)	
Dhb14	9.07		6.64	1.83	
	(9.08)		(6.65)	(1.88)	
Thr15	8.18	4.39	5.38	1.43	
	(8.18)	(4.40)	(5.37)	(1.43)	
Ala16	7.91	4.22	1.57		
	(7.92)	(4.21)	(1.58)		
A_2bu17	9.07	4.07	2.53, 2.38	3.13	NH2 = 7.81
	(9.10)	(4.07)	(2.55, 2.37)	(3.14)	(7.81)
A2bμ18	8.20	4.00	2.40	3.10	NH2 = 7.66
	(8.20)	(4.04)	(2.43)	(3.12)	(7.68)
Phe19	7.90	4.89	2.94, 3.43		7.38
	(7.90)	(4.89)	(3.44, 2.95)		(7.38)

dipolar connectivities (NOEs) which indicated the through-space proximity of the residues' protons. The fingerprint region of the two ROESY spectra obtained in aqueous 50 and 80% trifluoroethanol solutions are reported in Fig. 3A and B, respectively.

These results allowed sequence specific assignment along the peptide chain. The lack of the NH proton of the Pro2 residue was overcome by observing the NOEs of $C\delta H_2$ protons with the preceeding CαH, thus obtaining the step in the sequential assignment. The complete assignment for the two experimental conditions is reported in Table 2. Only small differences in chemical shifts were observed between spectra in 50 and 80% aqueous/trifluoroethanol.

Several inter-residue NOEs, detected in ROESY spectra at 0.3 s mixing time, have been observed and, after integration, classified by their intensity as weak, medium and strong. These experimental NOE data obtained in 50 and 80% trifluoroethanol are reported in Tables 3 and 4, respectively; these results were used as constraints in the computer simulations. The NOEs observed in both the ROESY spectra are overall similar in 50 and 80% trifluoroethanol and only small changes were found in some long range NOEs. Thus, the results obtained in 80% trifluoroethanol were chosen as the experimental starting data set for the molecular simulation whereas those obtained in 50% aqueous trifluoroethanol were used for checking controls.

Computer simulations

Distance geometry-simulated annealing. NOE restraints as derived from NMR data were included in the DG-SA computations. A total of 148 distance constraints, derived

Table 3. Inter-residual NOEs observed in the ROESY spectrum of Fuscopeptin B in 50% aqueous trifluoroethanol. Mixing time = 0.080 s, obtained as reported in Materials and methods. Symbols w, m and s refer to the integrated intensities as weak, medium and strong.

NH–NH		NH–CHα,β,γ,δ		Others	
Atom pair	Intensity	Atom pair	Intensity	Atom pair	Intensity
1N–2CδH	w	1CβH–2δCH	m		
2CδH–3N	w	2CδH–3CβH	w		
		2CαH–6CβH	w		
3N–4N	w	3CαH–4N	w		
		5CαH–4N	w		
5N–6N	m	5N–6CαH	m/w	6CαH–8CβH	m/w
		7CαH–8N	w	8CαH–11CβH	w
9N–10N	m/w	9CαH–10N	m		
11N–12N	m	11CαH–12N	w		
		11CβH–12N	m/w		
12N–13N	w	12N–13CαH	w		
		12CβH–13N	m/w		
13N–14N	w	13N–16CαH	w	13CγH–16CαH	w
		13CγH–17N	w		
14N–15N	m/w	13CαH–14N	w		
15N–16N	s	15CαH–16N	m/w	15CβH–16CαH	m
		15CβH–16N	m/s		
16N–17N	w	16CβH–17N	m/s		
		18CαH–19N	m/w	18CβH–19CγH	m/w
		18CγH–19N	w		

from 98 intra-residual and 50 inter-residual NOEs shown in Table 4, were used to generate 50 structures. A set of 34 structures with the lowest total energies were chosen to represent the solution conformation of fuscopeptin B.

All acceptance criteria [no NOE violations greater than 0.05 nm, no dihedral angle violations greater than 5°, root mean square deviation (rmsd) for bond deviations from ideality less than 0.001 nm, rmsd for angle deviations from ideality less than 2°] were fullfilled. The rmsd of the NOE violations of all of the structures was 0.003 ± 0.001 nm. The maximum violation was 0.004 nm. The rmsd of angles and improper dihedrals were 0.034 ± 0.002° and 0.030 ± 0.002°.

The backbone pair-wise rmsd for the 34 structures was 0.4 ± 0.1 (all heavy atoms 0.5 ± 0.1 nm) over the whole molecule, and the average rmsd to the mean structure were 0.3 ± 0.1 and 0.4 ± 0.1 nm, respectively. This result indicates a conformational heterogeneity of the structures. These findings made it impossible to select a unique representative structure with which to perform molecular dynamics simulations, or to group structures into a few classes on the basis of conformational similarity. Nevertheless, an examination of the ensemble led to the identification local elements of secondary structure preferentially adopted by the 34 conformers. Due to the presence of residues with alternating chirality, producing a conformational preference for turns [22], a tendency toward folded structures was evident. Beta and γ-turns can be identified, despite the fact that ϕ/ψ angular values at positions $i + 1$ and $i + 2$ are frequently inconsistent with classical turns; in a few cases it was not easy to distinguish type I′ from type III′ β-turns [23]. The hydrogen bond pattern of the ensemble shows that some hydrogen bonds occur more frequently than others: in all cases they contribute to the stabilization of the turns. The analysis of the ensemble shows that the conformation of fuscopeptin B can be described as being composed of two almost well-defined regions, a loop from Dhb1 to Ala5 and

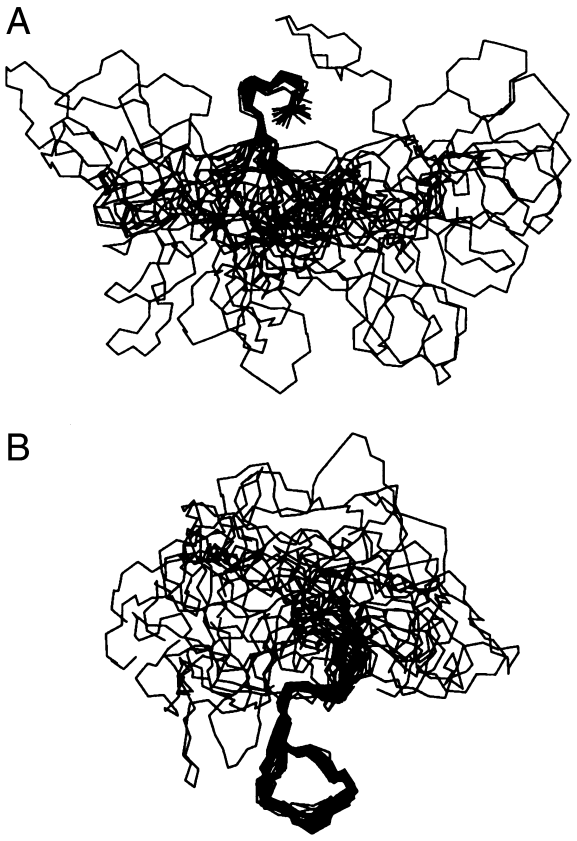

Fig. 4. The 34 structures of fuscopeptin B obtained after distance geometry-simulated annealing calculations. (A) Structures aligned from Dhb1 to Ala5; (B) structures aligned from Val13 to Phe19. Only backbone atoms N,Cα,C of the peptide moiety are shown.

Table 4. Inter-residual NOEs observed in the ROESY spectrum of fuscopeptin B in 80% aqueous trifluoroethanol. Mixing time of 0.080 s obtained as reported in Materials and methods. Symbols w, m and s refer to the integrated intensities as weak, medium and strong. FA, fatty acid.

NH-NH		NH–CHα,β,γ,δ		Others	
Atom pair	Intensity	Atom pair	Intensity	Atom pair	Intensity
				1N–C2H (FA)	s
				C5H (FA)–14CγH	w
				C7H (FA)–14CγH	w
1N–2CδH	m	1CHβ–2CδH	m		
2CδH–3N	m/w	2CδH–3CβH	w		
3N–4N	w	3N–5CαH	m/w		
		3CβH–5N	w		
		4CαH–5N	m		
		4CβH–5N	s		
5N–6N	w	6CαH–9N	w	5CαH–6CβH	w
7N–8N	m/s	7CαH–8N	m/w		
		8CαH–11N	w	8CβH–9CαH	m/w
				8Cγ′H–9CαH	m/w
9N–10N	m/w	9N–10CαH	w		
		9CαH–10N	m/s		
		9CαH–12N	m/w		
		10CαH–11N	s		
		10CβH–11N	w		
11N–12N	m/s	11CαH–12N	m	11Cγ′H–12CαH	ww
		11CβH–12N	m		
		11CαH–14N	m/w		
12N–13N	w	12N–13CαH	w	12CαH–13CβH	m/w
		12CαH–13N	s		
		12CβH–13N	m/s		
13N–14N	m/s	13CαH–14N	m/w		
		13CαH–16N	w-		
14N–15N	w				
15N–16N	s	15CαH–16N	w	15CβH–16CαH	w
		15CβH–16N	s		
		15CγH–16N	w		
16N–17N	w	16CβH–17N	s	16CβH–17γCH	m/w
		18CαH–19N	m/s		
		18βCH–19N	w		

the region from Val13 to Phe19 that includes the lactone ring. These are connected by a helical region with some conformational flexibility, from Ala6 to Ala12. Fig. 4A shows the ensemble of structures aligned from Dhb1 to Ala5; Fig. 4B shows the ensemble of structure aligned from Val13 to Phe19.

The fatty acid chain of the molecule is highly flexible, in agreement with the experimentally observed presence of only three NOE contacts involving it. This observation led us to consider the solution conformation of the peptidic region of fuscopeptin B; this is strictly valid for fuscopeptin A which differs only for the length of the fatty acid chain.

Almost all of the conformers have ϕ and ψ angles of residues 2–4 in the same region of the Ramachandran plot; residue 1 assumes two major values and residue 5 shows a wider range of values (Fig. 5A). The backbone rmsd of the average structure is 0.06 ± 0.02 nm with values ranging from 0.04 to 0.11 nm (all heavy atoms rmsd: 0.10 ± 0.04 nm). The majority of the conformers adopts a type IV β-turn conformation [24] from residues Pro2 to Ala5 (27 conformers) (Fig. 6A).

The second region with a defined secondary structure involves residues Val13 and Dhb14 of the chain, and residues Thr15 to Phe19, which form the lactone ring. The backbone shows some fluctuations at the lactonic closure and an inversion of 180° of the backbone amide bond between 2,4-diaminobutanoic acid (A_2bu)17 and A_2bu18. Almost all of the conformers have the ϕ and ψ angles of residues 15 and 16 and the ϕ angle of residue 19 in the same region of the Ramachandran plot. Residues 13, 14, 17 and 18 show spreading around two major values; ψ of residue 19 shows a wide variability (see Fig. 5B). Backbone rmsd of the average structure was 0.05 ± 0.01 nm with values ranging from 0.03 to 0.07 nm (all heavy atoms rmsd: 0.13 ± 0.03 nm). Three main turns characterize this region: an inverse γ-turn between Ala16 and A_2bu18 (25 conformers), stabilized by a hydrogen bond in 17 out of 25 conformers (Fig. 6G), a γ-turn between A_2bu17 and Phe19 (15 conformers), stabilized by a hydrogen bond in nine out of 18 conformers (Fig. 6H) and a β-turn between Val 13 and Ala16 (13 conformers) of type I′ or III′ (Fig. 6F), stabilized by a hydrogen bond in eight out of 15 conformers. Seven structures adopt a type III β-turn between residues Thr15 and A_2bu18 and seven structures have an inverse γ-turn between residues Val13 and Thr15 that is stabilized by a hydrogen bond in five.

A third structured region present between those previously described includes residues from Ala6 to Ala12 and is characterized by some conformational variability and an rmsd

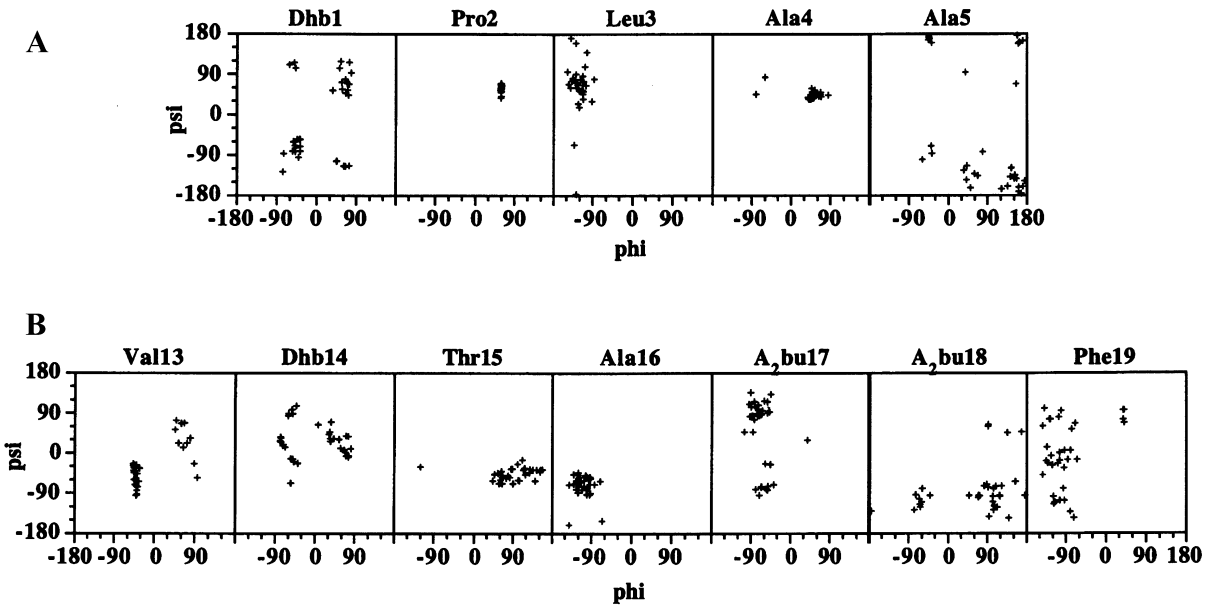

Fig. 5. Ramachandran plot of the conformers found in DG-SA molecular simulation of Fuscopeptin B. (A) Residues from Dhb1 to Ala5; (B) residues from Val13 to Phe19.

for the backbone of 0.15 ± 0.05 nm with values ranging from 0.09 to 0.27 nm (nonhydrogen atoms rmsd: 0.2 ± 0.06 nm). In this region it was possible to identify structures with segments of distorted and nonsuperimposable left-handed α-helicity. About 10 structures show such feature between residues 7 and 12 as shown in Fig. 7A,B. This region is probably the structured part of the molecule which in 80% aqueous trifluoroethanol is responsible for the CD spectrum reported in Fig. 2. In this region, experimental NMR data are compatible also with other conformations. Other conformers show four consecutive turns: two β-turns, from Ala6 to Ala12 (11 conformers) and from Gly9 to Ala12 (nine conformers) which both could be described as type I′ or III'; two β-turns of type I′ from residue 7 to 10 (12 conformers) and from Val8 to Val11 (11 conformers) as reported in Fig. 6B–E.

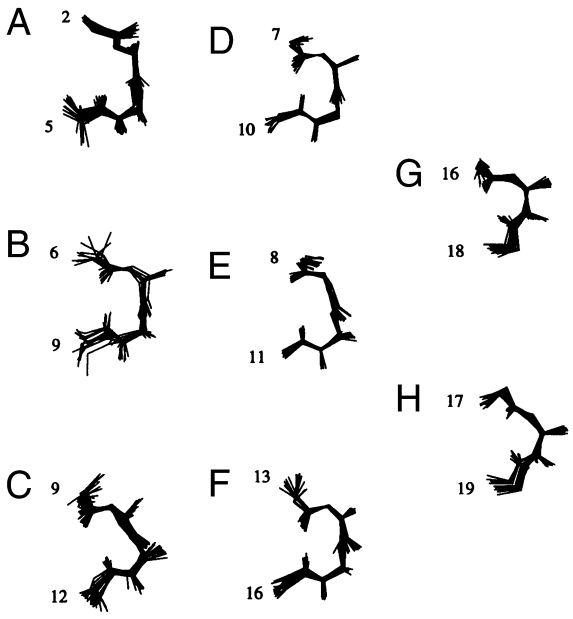

Fig. 6. Prevalent turns present in fuscopeptin B. (A–F) β-turns; (G–H) γ-turns. Atoms N, Cα, C, O, HN of residue *i* and Cβ of residue (*i* + 2) are shown.

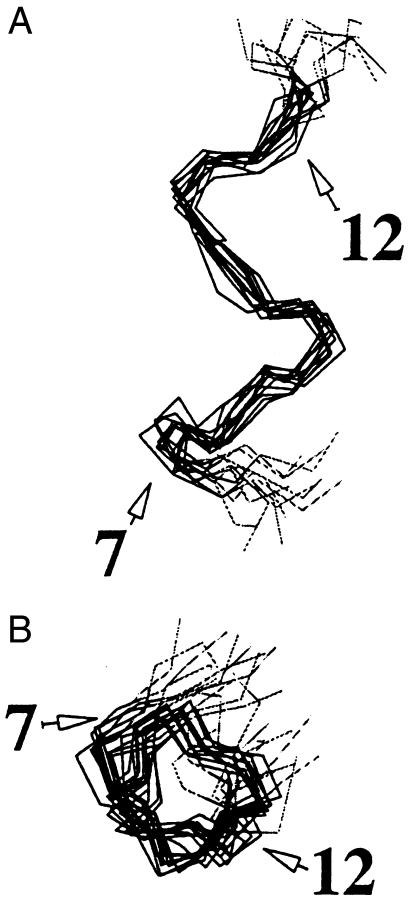

Fig. 7. Structural region of fuscopeptin B from Ala7 to Ala13. (A) Side view; (B) top view. Only backbone atoms N,Cα,C are shown.

Finally the torsion angle of the lactonic ring closure assumes an almost *trans* conformation in all conformers.

The results reported here are precise for the backbone chain only because of the relatively small number of NOE constraints reported in Tables 3 and 4. Because of the small number of constraints the side chains remain largely undetermined.

DISCUSSION

The bioactive lipodepsipeptides fuscopeptin A and fuscopeptin B are structurally related to some pseudomonad metabolites studied previously. In particular they share with tolaasins, syringopeptin 22, syringopeptin 25A and corpeptins a 3-hydroxy substituted unbranched fatty acid chain and a long hydrophobic peptide moiety with a positively charged cyclized C terminus. The cyclized moiety is formed by eight amino acid residues in syringopeptins and by five residues in all of the others.

The solution structure of fuscopeptin B, and consequently that of fuscopeptin A, which only differs in its slightly shorter 3-hydroxy fatty acid moiety, has been elucidated by NMR spectroscopy and molecular simulations using DG-SA methods, with the use of NOE data collected from fully assigned two-dimensional NMR spectra.

The comparison of secondary structural elements of fuscopeptins with those of syringopeptin 25A [6] shows the occurrence in both products of three comparable structural motifs presenting hydrogen bonds in the same regions.

Two consecutives turns (an inverse γ-turn and a type I′ β-turn) occur between residues in the N-terminal region of syringopeptin 25A; they have their analogy in the preference for a type IV β-turn in the same position of conformers of fuscopeptins.

The aromatic character of the C-terminal residue found in syringopeptins and syringotoxin is mantained in fuscopeptins and the nature of the hydroxy-amino acid residue (D-*allo*-Thr) – where the cyclic closure occurs preceeded by a conserved Dhb residue. A γ-turn, involving the C-terminal sequence, and other two nonclassified β-turns, all stabilized by hydrogen bonds, form the structural pattern of the lactone ring of syringopeptin 25A. This structural motif has its analogy in the preference of most of the 34 conformers of fuscopeptins for a γ-turn at the C terminus, consecutive to an inverse γ-turn; in most cases both are stabilized by a hydrogen bond.

A different structure has been also found for the central region. In fact, the higher content of the dehydro residue Dhb in syringopeptin 25A as compared with fuscopeptins confers a higher conformational rigidity in its central region. On the contrary, the consecutive presence of D-amino acids in fuscopeptins is probably responsible for the assumption of a left-handed α-helicoidal conformation in aqueous trifluoroethanol as by CD spectroscopy.

The conformation of the lactone ring is similar to that found in the two 'small' lipodepsipeptides syringotoxin [20] and pseudomycin A [19] as well as in syringopeptin 25A. This conformation, resembling the seam of a tennis ball, was found for the first time in the bioactive lipodepsinonapeptide WLIP: white line inducing principle, produced by *Pseudomonas reactans* [25]. A motif of two consecutive hydrogen-bonded turns (see Fig. 8) was previously observed in the lactone macrocycle of pseudomycin A [19].

The effect of the aqueous trifluoroethanol solvent, which certainly constitutes an aid to the structural studies by NMR in solution, is also proof that these compounds, with exception of syringopeptin 25A, are mainly unstructured or only partly structured in water and become more more structured in this solvent mixture which is a membrane-like environment. This is in line with the membrane perturbing properties of these lipodepsipeptides. The complete correlation between the structure in solution and the bioactive properties of these compounds is not understood completely and awaits the study of a more complete set of similar phytotoxins from different sources. In fact, the effect of the fatty acid chain, the hydrophobic elements, the balance of polar/hydrophobic residues in the sequence, the role of alternating chiralities and, finally, the lactonic closure on the solution conformation – and consequently the biological properties – of these phytotoxins has not been clarified completely.

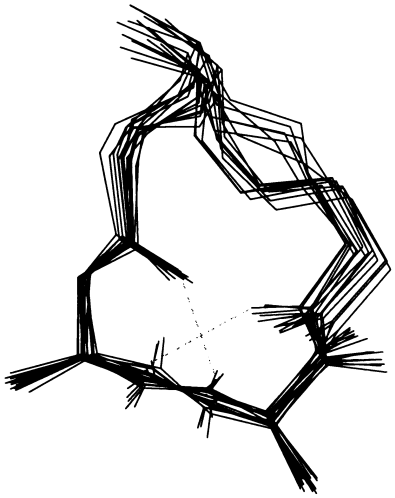

Fig. 8. View of the lactone ring of fuscopeptin B with two consecutive γ-turns. Dashed lines connect HN and O atoms involved in a hydrogen bond in most of the structures.

ACKNOWLEDGEMENTS

This research was partly supported by the National research project (PRIN) 'Biologia Strutturale' of the Ministero della Universita′ Ricerca Scientifica e Tecnologica (MURST) and by the target project of the Italian Research Council (CNR) 'Biotecnologie'.

REFERENCES

1. Emanuele, M.C., Scaloni, A., Lavermicocca, P., Jacobellis, N.S., Camoni, L., Di Giorgio, D., Pucci, P., Paci, M., Segre, A. & Ballio, A. (1998) Corpeptins, new bioactive lipodepsipeptides from cultures of *Pseudomonas corrugata. FEBS Lett.* **433**, 317–320.
2. Flamand, M.C., Pelsser, S., Ewbank, E. & Maraite, H. (1996) Production of syringotoxin and other bioactive peptides by *Pseudomonas fuscovaginae*. *Physiol. Mol. Plant Pathol.* **48**, 217–231.
3. Ballio, A., Bossa, F., Camoni, F., Di Giorgio, D., Flamand, M.-C., Maraite, H., Nitti, G., Pucci, P. & Scaloni, A. (1996) Structure of Fuscopeptins, phytotoxic metabolites of *Pseudomonas fuscovaginae*. *FEBS Lett.* **381**, 213–216.
4. Nutkins, J.C., Mortishire-Smith, R.J., Packman, L.C., Brodey, C.L., Rainey, P.B., Johnstone, K. & Williams, D.H. (1991) Structure determination of tolaasin, an extracellular lipodepsipeptide produced by the mushroom pathogen *Pseudomonas tolaasii* Paine. *J. Am. Chem. Soc.* **113**, 2621–2627.
5. Ballio, A., Barra, D., Bossa, F., Collina, A., Grgurina, I., Marino, G., Moneti, G., Paci, M., Pucci, P., Segre, A.L. & Simmaco, M. (1991) Syringopeptins, new phytotoxic lipodepsipeptides of *Pseudomonas syringae* pv. *syringae. FEBS Lett.* **291**, 109–112.

6. Ballio, A., Bossa, F., Di Giorgio, D., Di Nola, A., Manetti, C., Paci, M., Scaloni, A. & Segre, A.L. (1995) Solution conformation of the *Pseudomonas syringae* pv. *syringae*, phytotoxic lipodepsipeptide SP25-A: two-dimensional NMR, distance geometry and molecular dynamics. *Eur. J. Biochem.* **234**, 747–758.
7. Braunschweiler, L. & Ernst, R.R. (1983) Coherence transfer by isotopic mixing: application to proton correlation spectroscopy. *J. Magn. Res.* **53**, 521–528.
8. Bothner-By, A.A., Stephens, R.L. & Lee, J. (1984) Structure determination of a tetrasaccharide: transient nuclear Overhauser effects in the rotating frame. *J. Am. Chem. Soc.* **106**, 811–813.
9. Hwang, T. & Shaka, A.J. (1992) Cross relaxation without TOCSY: transverse rotating frame Overhauser effect spectroscopy. *J. Am. Chem. Soc.* **114**, 3157–3159.
10. Marion, D. & Wutrich, K. (1983) Application of phase sensitive two-dimensional correlated spectroscopy (COSY) for measuraments of 1H–1H spin–spin coupling costants in proteins. *Biochem. Biophys. Res. Commun.* **113**, 967–974.
11. Bax, A. & Davis, D.G. (1985) MLEV-17 based two-dimensional homonuclear magnetization transfer spectroscopy. *J. Magn. Res.* **65**, 355–360.
12. Brünger, A.T. (1988) *X-PLOR 3.1 Manual*. Yale University, New Haven, CT.
13. Kirkpatrick, S., Gelatt, C.D. Jr & Vecchi, M.P. (1983) Optimization by simulated annealing. *Science* **220**, 671–680.
14. Wagner, G., Braun, W., Havel, T.F., Schaumann, T., Go, N. & Wüthrich, K. (1987) Protein structure in solution by nuclear magnetic resonance and distance geometry. The polypeptide fold of the basic pancreatic trypsin inhibitor determined using two different algorithms, DISGEO and DISMAN. *J. Mol. Biol.* **196**, 611–640.
15. Nilges, M., Clore, M.G. & Gronenborn, A.M. (1988) Determination of three-dimensional structures of proteins from interproton distance data by hybrid distance geometry-dynamical simulated annealing calculations. *FEBS Lett.* **229**, 317–324.
16. Brooks, C.L. & Karplus, M. (1983) Deformable stochastic boundaries in molecular dynamics. *J. Chem. Phys.* **79**, 6312–6325.
17. MacKerell, A.D., Jr, Bashford, D., Bellott, M., Dunbrack, R.L., Jr, Field, M.J., Fischer, S., Gao, J., Guo, H., Ha, S., Joseph, D., Kuchnir, L., Kuczera, K., Lau, F.T.K., Mattos, C., Michnick, S., Ngo, T., Nguyen, D.T., Prodhom, B., Roux, B., Schlenkrich, M., Smith, J.C., Stote, R., Straub, J., Wiorkiewicz-Kuczera, J. & Karplus, M. (1992) Self consistent parametrization of biomolecules for molecular modeling and condensed phase simulations. *FASEB J.* **6**, A143.
18. Kaptein, R., Boelens, R., Scheek, R.M. & van Gunsteren, W.F. (1988) Protein structures from NMR. *Biochemistry* **27**, 5389–5395.
19. Coiro, V.M., Segre, A.L., Di Nola, A., Paci, M., Grottesi, A., Veglia, G. & Ballio, A. (1998) Solution conformation of the *Pseudomonas syringae* MSU 16H phytotoxic lipodepsipeptide pseudomycin A determined by computer simulations using distance geometry and molecular dynamics from NMR data. *Eur. J. Biochem.* **257**, 449–456.
20. Ballio, A., Collina, A., Di Nola, A., Manetti, C., Paci, M. & Segre, A.L. (1994) Determination of structure and conformation in solution of syringotoxin, a lipodepsipeptide from *Pseudomonas syringae* pv. *syringae* by 2D NMR and molecular dynamics. *Struct. Chem.* **5**, 43–50.
21. Powell, M.J.D. (1977) Restart procedures for the conjugate gradient method. *Math. Prog.* **12**, 241–254.
22. Wilmot, C., M. & and Thornton, J.M. (1988) Analysis and prediction of different types of β-turns in proteins. *J. Mol. Biol.* **203**, 221–232.
23. Rose, G.D., Gierasch, L.M. & Smith, J.A. (1985) Turns in peptides and proteins. *Adv. Protein Chem.* **37**, 1–109.
24. Lewis, P.N., Momany, F.A. & Scheraga, H.A. (1973) Chain reversals in proteins. *Biochim. Biophys. Acta* **303**, 211–229.
25. Mortishire-Smith, R.J., Nutkins, J.C., Packman, L.C., Brodey, C.L., Rainey, P.B., Johnstone, K. & Williams, D.H. (1991) Determination of the structure of an extracellular peptide produced by the mushroom saprotroph *Pseudomonas reactans*. *Tetrahedron* **47**, 3645–3654.
26. Barra, D. & Simmaco, M. (1995) Amphibian skin: a promising resource for antimicrobial peptides. *Trends Biotech.* **13**, 205–209.
27. Isogai, A., Iguchi, H., Nakayama, J., Kusai, A., Takemoto, J.Y. & Suzuki, A. (1995) Structural analysis of new syringopeptins by tandem mass spectrometry. *Biosci. Biotechnol. Biochem.* **59**, 1374–1376.